NIH Public Access
Author Manuscript
Osteoarthritis Cartilage. Author manuscript; available in PMC 2013 January 25.

Published in final edited form as:
Osteoarthritis Cartilage. 2011 February ; 19(2): 200–205. doi:10.1016/j.joca.2010.11.005.

Intrinsic repair of full-thickness articular cartilage defects in the axolotl salamander

R.S. Cosden[†], **C. Lattermann**[‡], **S. Romine**[‡], **J. Gao**[§], **S.R. Voss**[‖], and **J.N. MacLeod**[†,‡,*]

[†]Department of Veterinary Science, University of Kentucky, Lexington, KY, USA

[‡]Department of Orthopaedic Surgery, University of Kentucky, Lexington, KY, USA

[§]Department of Computer Science, University of Kentucky, Lexington, KY, USA

[‖]Department of Biology, University of Kentucky, Lexington, KY, USA

SUMMARY

Objective—The ability to fully regenerate lost limbs has made the axolotl salamander (*Ambystoma mexicanum*) a valuable model for studies of tissue regeneration. The current experiments investigate the ability of these vertebrates to repair large articular cartilage defects and restore normal hyaline cartilage and joint structure independent of limb amputation.

Methods—Full-thickness articular cartilage defects were made by resection of the medial femoral condyle to the level of the metaphysis. At 0, 2 days, 1, 2, 3, 4, 6, 8, 12, 18, 24, 36 and 48 weeks post-surgery, the repair process was analyzed on H&E and Safranin-O stained 7 μm tissue sections. Symmetric Kullback–Leibler (SKL) divergences were used to assess proteoglycan staining intensities. Immunohistochemistry was performed for collagen types I and II.

Results—A fibrous “interzone-like” tissue occupies the intraarticular space of the axolotl femorotibial joint and no evidence of joint cavitation was observed. By 4 weeks post-surgery, cells within the defect site exhibited morphological similarities to those of the interzone-like tissue. At 24 weeks, joint structure and cartilaginous tissue repair were confirmed by immunohistochemistry for collagen types I and II. Quantitation of Safranin-O staining indicated restoration of proteoglycan content by 18 weeks.

Conclusions—The axolotl femorotibial joint has morphological similarities to the developing mammalian diarthrodial joint. Cells in the intraarticular space may be homologous to the interzone tissue and contribute to intrinsic repair of full-thickness articular cartilage defects. Taken together, these results suggest that the axolotl may serve as a valuable model for the investigation of cellular and molecular mechanisms that achieve full articular cartilage repair.

[*]Address correspondence and reprint requests to: J.N. MacLeod, University of Kentucky, Department of Veterinary Science, 108 Gluck Equine Research Center, Lexington, KY 40546, USA. Tel: 1-859-257-4757; Fax: 1-859-257-8942. JNMacl2@uky.edu (J.N. MacLeod)..

Contributions

Rebekah Cosden: design of the study, acquisition of the data, analysis and interpretation, drafting and revising of the article and final approval.
Christian Lattermann: design of the study, analysis and interpretation, revising of the article and final approval.
Spencer Romine: design of the study, revising of the article and final approval.
Jizhou Gao: SKL data acquisition and analysis, revising of the article and final approval.
S. Randal Voss: analysis and interpretation of data, revising of the article and final approval.
James N. Macleod: design of the study, analysis and interpretation, drafting and revising of the article and final approval.

Conflict of interest

All authors declare no conflict of interest.

Keywords

Articular cartilage repair; Amphibian; Joint interzone; Axolotl salamander

Introduction

Pain, loss of mobility, and osteoarthritis resulting from injured articular cartilage are troublesome for patients and clinicians alike. The intrinsic repair capacity of mammalian articular cartilage is extremely limited, making therapeutic treatment of articular cartilage injury challenging[1,2]. Despite recent advances in surgical and pharmacological treatment options, damaged adult articular cartilage is never fully restored[3]. Instead, a structurally different and functionally deficient “hyaline-like” scar tissue forms in place of preexisting articular cartilage[4–6]. There are limited data suggesting that fetal or very young mammals may be able to heal partial thickness articular cartilage lesions without scar formation, but this ability appears to be lost with ambulation and cartilage maturation in the postnatal period[7–9]. Thus, a better understanding of joint morphogenesis and tissue patterning may be useful in developing successful articular cartilage repair strategies[10]. An interesting model system for cartilage development is found in the remarkable tissue regenerative capabilities of urodele amphibians. For example, the Mexican axolotl salamander (*Ambystoma mexicanum*) retains the ability to regenerate any of its four well-defined limbs throughout its lifespan. After limb amputation, a blastema forms and serves as a source of cells and paracrine factors participating in regeneration of the limb through a process that recapitulates embryonic limb development[11,12]. Investigation of limb development and regeneration in urodeles may provide insight into tissue repair mechanisms that have been lost or are no longer fully utilized in mammals.

Despite the extraordinary regenerative capabilities of the axolotl salamander, the capacity for intrinsic tissue repair of musculoskeletal defects in the absence of amputation and blastema formation has limits. As with mammals, axolotls are not able to heal bone defects of critical dimension[13,14]. While nondisplaced fracture repair in the axolotl occurs through mechanisms similar to those found in mammals, their ability to repair articular cartilage defects is unknown. The objective of these experiments was to investigate the utility of the axolotl as a vertebrate model to study articular cartilage repair independent of limb amputation. We hypothesized that these salamanders possess the intrinsic ability to repair large full-thickness lesions in the articular cartilage of the distal femur.

Materials and methods

Animals

Axolotl salamanders (*A. mexicanum*) were obtained from the Ambystoma Genetic Stock Center (Lexington, KY) as fertilized embryos. Axolotls were housed individually at 20–22°C in 25% Holtfreter's solution[15]. Larvae were fed freshly hatched brine shrimp (Artemia sp., Aquatic Ecosystems, Apopka, FL) until approximately 4 cm in length, after which they were fed California blackworms (*Lumbriculus* sp., J.F. Enterprises, Oakdale, CA). All procedures were conducted in accordance with a University of Kentucky institutional animal care and use protocol (IACUC #2008-0282).

Surgical procedures

Unilateral femorotibial joint surgery was performed on a total of 72 axolotl salamanders at 4 months of age with a body length of approximately 6–8 cm. A surgical plane of anesthesia was achieved by immersion in 0.01% benzocaine (w/v, Sigma, Cat. #E1501, St. Louis, MO)

in Holtfreter's solution. Anesthesia was maintained by wrapping the animals in a towel soaked in the same benzocaine solution throughout the procedure. The knee joint was positioned in a flexed position and supported from underneath during the surgery. A femorotibial joint arthrotomy was performed through a 5–8 mm skin incision [Fig. 1(A)], which was held retracted using two 21 gauge needles. The medial femoral condyle was identified and resected to the level of the metaphysis [Fig. 1(B)]. The skin incision was then closed using 10–0 vicryl suture (Covidien, Cat. #N2736K, Mansfield, MA). The salamanders were recovered from anesthesia in Holtfreter's solution.

Sample collection

Axolotls were sacrificed at post-surgical timepoints of 0 (n=4), 2 days (n= 6), 1 week (n=6), 2 weeks (n= 6), 3 weeks (n= 6), 4 weeks (n= 6), 6 weeks (n= 6), 8 weeks (n =12), 12 weeks (n=10), 18 weeks (n= 4), 24 weeks (n=2), 36 weeks (n=2), and 48 weeks (n= 2). Salamanders were deeply anaesthetized with 0.01% benzocaine prior to euthanasia performed by cervical dislocation. Operated and contralateral control limbs were fixed in 4% paraformaldehyde in phosphate buffered saline (PBS) for 48 h, decalcified in ethylenediaminetetraacetic acid (EDTA) and hydrochloric acid (Richard Allen Scientific, Kalamazoo, MI), and paraffin embedded. Samples were sectioned at 7 μm for all histological analyses.

Histology and immunohistochemistry

Hematoxylin and Eosin (H&E) staining was performed using established protocols. Safranin-O/Fast Green staining was optimized and standardized for axolotl samples using aqueous 0.001% Fast Green and 0.05% Safranin-O solutions. Immunostaining was performed using standard avidin–biotin complex reagents and methods according to the manufacturer's protocol (Santa Cruz Biotechnology, Cat. #sc2017, sc2019, Santa Cruz, CA). Sections stained for type I collagen were pretreated to enhance antigen retrieval with a 0.2 M sodium citrate buffer, pH 3.5, for 20 min at 37°C. Polyclonal rabbit anti-rat collagen I IgG (Millipore, Cat. #AB755P, Billerica, MA) was diluted at 1:100 as the primary antibody. Type II collagen-stained sections were pretreated to enhance antigen retrieval with 1% pepsin in 10 mM HCl for 10 min at 37°C. Monoclonal mouse anti-chicken collagen II IgG (Millipore, Cat. #MAB8887) was diluted at 1:800 as the primary antibody. All sections were counterstained with Gill No.3 hematoxylin (Sigma, Cat#HS316). Sections of normal equine subchondral bone and articular cartilage were used as positive controls for type I and type II collagen immunostaining, respectively, using the same hybridization reagents and protocols. Negative controls for each assay included omission of the primary or secondary antibody from the immunostaining protocol.

Safranin-O staining image analyses

Safranin-O staining intensity may be used to measure total proteoglycan content of cartilage sections, as the dye binds stoichiometrically to negatively charged proteoglycans[16]. To quantify staining intensity of Safranin-O stained sections, digital images were analyzed using MatLab software (The Mathworks, Natick, MA). For each sample, a region within the lesion site [Fig. 2(A,1)] was selected for comparison to a region of normal cartilage in the lateral control condyle [Fig. 2(A,2)]. Red pixels within each region were grouped into 64 bins along a 256 color palette, and histograms displaying normalized pixel distributions were generated [Fig. 2(B)–(C)].

The Kullback–Leibler divergence (KL divergence) was used to compare pixel distributions between each site. The KL divergence is a dissimilarity measure between two arbitrary probability distributions[17,18]. Given two distributions P and Q, their KL divergence is defined to be

$$\mathrm{KL}(P, Q) = \int_{-\infty}^{\infty} p(x) \log \frac{p(x)}{q(x)} \mathrm{d}x.$$

The KL divergence is always non-negative, and KL(*P, Q*)=0 if and only if *P*= *Q*. Therefore, as the staining intensity of the lesion site (*P*) approaches that of the normal cartilage (*Q*), the KL divergence will approach 0.

Symmetric Kullback–Leibler (SKL) divergence [SKL(*P, Q*) =½ KL (*P, Q*) +½ KL(*Q, P*)] was computed between two histograms from each sample. As the logarithm of the SKL can be approximately treated as normally distributed, a parametric one-way ANOVA was applied to the $\log_{10}(\mathrm{SKL})$[19]. Tukey–Kramer analysis was performed to allow for comparison of unequally sized groups at each post-surgical collection point. All statistical tests were performed using Intercooled Stata (Statacorp LP, College Station, Texas). Differences were considered significant at $P < 0.05$.

Results

Knee joint anatomy

As in all vertebrates, the knee joint in the axolotl is formed by the articulation of the distal femur with the proximal tibia and fibula (Fig. 1). The fibula articulates with the lateral femoral condyle directly and is part of the weight-bearing surface. The femorotibial joint comprises approximately two thirds of the articulating surface, with the femorofibular joint comprising the remaining third [Fig. 3(A)]. Axolotls lack the patella sesamoid. Grossly, the articulating surface appears translucent and cartilaginous.

Histological evaluation revealed cartilage on both the distal femur and proximal tibial and fibular articular surfaces. A rim of cortical bone surrounds the diaphysis and metaphysis, but there was no evidence of a secondary ossification center and the epiphysis appeared entirely cartilaginous. The epiphyseal/articular cartilage in axolotls contained chondrocytes that measure approximately 10–20 μm in diameter with an isotropic distribution. Chondrocytes in the metaphysis were larger, measuring roughly 25–35 μm in diameter and organized in clusters [Fig. 3(B)]. No evidence of a meniscus or intraarticular ligaments was observed. Instead, a fibrous “interzone-like” tissue occupied the entire intraarticular space, with cells that appeared adherent to the articular surfaces [Fig. 3(C)]. There was no evidence of joint cavitation.

Red coloration of Safranin-O/Fast Green stained samples indicates high proteoglycan content throughout the cartilage. Faint staining is also present in the interzone [Fig. 3(D)]. Type I collagen expression is found in the interzone-like tissue and cortical bone [Fig. 3(E)]. Immunostaining of type II collagen indicates uniform expression throughout the epiphyseal/articular cartilage. There is a marked decrease in type II collagen staining above the epiphyseal/metaphyseal junction [Fig. 3(F)].

Repair of structural lesions in the distal femur

Arthrotomy and surgical resection of the medial femoral condyle was accomplished reproducibly and without post-surgical complications. Resection to the level of the metaphysis was confirmed histologically at day 0 [Fig. 4(A)]. The healing response was evaluated sequentially over a total of 48 weeks. At the 2-day and 1-week [Fig. 4(B)] timepoints, the lesion site was occupied primarily by nucleated erythrocytes. A limited number of neutrophils and lymphocytes were also present. In limbs collected 2–4 weeks after surgery [Fig. 4(C)–(D)], cells were observed in the lesion area with morphological

features ranging from interzone-like to more chondrocytic. These characteristics progressed during the period from 6–12 weeks, with the cells that exhibited a more chondrocyte-like morphology usually observed in the proximal portion of the lesion away from the articular surface, compared to repair tissue cells closer to the joint surface and interzone which were less organized [Fig. 4(E)–(G)]. At 18 weeks post-surgery [Fig. 4(H)], restoration of the medial condyle anatomy became increasingly apparent with interzone tissue more evenly distributed across the joint space. By 24 weeks, femorotibial joint structure approached normal with restoration of uniform chondrocyte morphology and isotropic cellular distribution across the epiphyseal/articular cartilage [Fig. 4 (I)]. There was minimal histological evidence of the medial condyle resection at the 24–48-week post-surgical timepoints.

Restoration of cartilaginous tissue at 24 weeks was confirmed by Safranin-O staining for proteoglycan content, as well as the immunohistochemical staining patterns for type I and type II collagen [Fig. 4(J)–(L)]. Restoration of proteoglycan levels within the defect site was confirmed by quantitative analysis of Safranin-O stained images (Fig. 5). There was a strong negative correlation between progressive post-surgical collection time and SKL, indicating that proteoglycan staining intensity and homogeneity of the normal articular cartilage and lesion sites became more similar as healing progressed (r=−0.89, P< 0.01).

Mean SKL values comparing normal and repair sites were not different (P >0.05) than in controls by 18 and 24 weeks, indicating comparable staining intensity and proteoglycan content in the two femoral condyles (Fig. 5).

Discussion

The results of this study indicate that the axolotl salamander has the ability to heal localized articular cartilage defects. While mammals form a fibrocartilage repair tissue in response to full-thickness cartilage lesions[5], it appears that the axolotl is able to fully restore articular structure and cartilage matrix components without scar formation.

Wound repair in mammals can be divided into three classic stages: inflammation, new tissue formation, and tissue remodeling. Fibrosis, the deposition of an excess of fibrous connective tissue, especially during the middle `tissue formation' stage of the healing process, is known to limit the restoration of normal structure and function following injury[20–22]. The axolotl's inflammatory response to injury may be less pronounced than typically seen in mammals, resulting in reduced fibrosis during the wound repair process[23]. Histological assessments of early post-surgical collection points revealed evidence of clot formation within the defect site and limited participation of inflammatory cells. There was no evidence of fibrotic tissue deposition into the wound site. Instead, cells with a morphological structure resembling those found within the interzone-like tissue appear to fill the defect site and either differentiate into or become replaced by chondrocytes. The identity and function of the interzone-like tissue is of particular interest, as it may contribute to true cartilage restoration without the fibrous inhibition which occurs in mammals.

Several observations have led us to hypothesize that the axolotl femorotibial joint has similarities to the developing synovial joint of a mammalian fetus. Unlike other urodele amphibians, the axolotl does not spontaneously undergo metamorphosis to a terrestrial adult form, but rather retains larval characteristics into sexually maturity[24,25]. As such, adult axolotls have neotenic characteristics, exhibiting external gills and fins while developing four well defined articulating limbs. Several structural features of the adult axolotl knee resemble those found in a developing mammalian diarthrodial joint prior to cavitation. The isotropic organization of chondrocytes within the axolotl articular/epiphyseal cartilage is

reminiscent of articular cartilage structure in the mammalian fetus and neonate[26–28]. During synovial joint development, the interzone forms as a flattened layer of cells connected by gap junctions after initial condensation of the prechondrogenic mesenchyme[29–31]. Cells from the interzone eventually differentiate into articular chondrocytes[32]. Interzone cells are similar in appearance to those found within the intraarticular space of the axolotl femorotibial joint, which also remain attached to the articular surface. If the intraarticular cells of the axolotl are indeed homologous to interzone cells in developing avian and mammalian synovial joints, they may maintain chondrogenic potential and be able to contribute to the repair of localized articular cartilage defects. Our histological observations suggest that these cells have a role in the repair process, but cell tracking and additional mechanistic experiments are needed to investigate this further.

The articular cartilage repair process in axolotls may also occur through molecular and cellular mechanisms similar to total limb regeneration. However, epimorphic limb regeneration requires that a blastema be in contact with the tissue stump[33–34]. Thus, closed skeletal defects likely heal through other mechanisms[35]. For example, the axolotl is able to heal simple bone fractures in a fashion similar to other vertebrates, and fails to heal bone fractures of critical dimension[13,14]. In the current study, no histological evidence of blastema formation was observed and we believe that the intrinsic repair of the resected medial condyle occurred by mechanisms distinct of regeneration. Taken together, these results suggest that the axolotl may serve as a valuable vertebrate model for the investigation of cellular and molecular mechanisms that achieve full articular cartilage repair.

Acknowledgments

Assistance from Dr Jinze Liu and Dr James Monaghan is graciously acknowledged.

Role of funding source

Financial support was received from the Gluck Equine Research Foundation and the University of Kentucky Department of Orthopaedic Surgery. These study sponsors were not involved in the study design, data collection or analysis; or in the writing of the manuscript. Furthermore, they did not affect the decision to submit the manuscript for publication.

References

1. Buckwalter JA, Mankin HJ. Instructional course lectures, the American academy of orthopaedic surgeons – Articular cartilage. Part II: degeneration and osteoarthrosis, repair, regeneration, and transplantation. J Bone Joint Surg Am. 1997; 79:612–32.
2. Ghadially FN, Thomas I, Oryschak AF, Lalonde JM. Long-term results of superficial defects in articular cartilage: a scanning electron-microscope study. J Pathol. 1977; 121:213–7. [PubMed: 874638]
3. Gerjo, JVMvO; Mats, B.; James, ED.; Yvonne, MB-J.; Reinhold, GE.; Yrjö, TK., et al. Cartilage repair: past and future; lessons for regenerative medicine. J Cell Mol Med. 2009; 13:792–810. [PubMed: 19453519]
4. Furukawa T, Eyre DR, Koide S, Glimcher MJ. Biochemical studies on repair cartilage resurfacing experimental defects in the rabbit knee. J Bone Joint Surg Am. 1980; 62:79–89. [PubMed: 7351420]
5. Mienaltowski MJ, Huang L, Frisbie DD, McIlwraith CW, Stromberg AJ, Bathke AC, et al. Transcriptional profiling differences for articular cartilage and repair tissue in equine joint surface lesions. BMC Med Genomics. 2009; 2:60. [PubMed: 19751507]
6. Mienaltowski MJ, Huang L, Bathke AC, Stromberg AJ, MacLeod JN. Transcriptional comparisons between equine articular repair tissue, neonatal cartilage, cultured chondrocytes and mesenchymal stromal cells. Brief Funct Genomics. May; 2010 9(3):238–50. [PubMed: 20348544]

7. Wagner W, Reichl J, Wehrmann M, Zenner HP. Neonatal rat cartilage has the capacity for tissue regeneration. Wound Repair Regen. 2001; 9:531–6. [PubMed: 11896996]
8. Namba RS, Meuli M, Sullivan KM, Le AX, Adzick NS. Spontaneous repair of superficial defects in articular cartilage in a fetal lamb model. J Bone Joint Surg Am. 1998; 80:4–10. [PubMed: 9469302]
9. Calandruccio RA, Gilmer WSJR. Proliferation, regeneration, and repair of articular cartilage of immature animals. J Bone Joint Surg Am. 1962; 44:431–55.
10. Tuan RS. Biology of developmental and regenerative skeletogenesis. Clin Orthop Relat Res. 2004; 427:S105–17. [PubMed: 15480052]
11. Tanaka EM. Regeneration: if they can do it, why can't we? Cell. 2003; 113:559–62. [PubMed: 12787496]
12. Holly LDN, Jo Ann C, Ellen AGC, David LS. Regeneration of the urodele limb: a review. Dev Dyn. 2003; 226:280–94. [PubMed: 12557206]
13. Hutchison C, Pilote M, Roy S. The axolotl limb: a model for bone development, regeneration and fracture healing. Bone. 2007; 40:45–56. [PubMed: 16920050]
14. Satoh A, Cummings GM, Bryant SV, Gardiner DM. Neurotrophic regulation of fibroblast dedifferentiation during limb skeletal regeneration in the axolotl (*Ambystoma mexicanum*). Dev Biol. 2010; 337:444–57. [PubMed: 19944088]
15. Duhon, S. Raising the axolotl in captivity. In: Malacinski, G.; Armstrong, J., editors. Developmental Biology of the Axolotl. Oxford University Press; New York: 1989. p. 220-7.
16. Rosenburg L. Chemical basis for the histological use of safranin O in the study of articular cartilage. J Bone Joint Surg. 1971; 53:69–82. [PubMed: 4250366]
17. Kullback S, Leibler RA. On information and sufficiency. Ann Math Stat. 1951; 22(1):79–86.
18. Pinsker, MS. Information and Information Stability of Random Variables and Processes. Holden-Day; San Francisco: 1964.
19. Shutin D, Zlobinskaya O. Application of information-theoretic measures to quantitative analysis of immunofluorescent microscope imaging. Comput Methods Programs Biomed. 2010; 97:114–29. [PubMed: 19570589]
20. Gurtner GC, Werner S, Barrandon Y, Longaker MT. Wound repair and regeneration. Nature. 2008; 453:314–21. [PubMed: 18480812]
21. Klapka N, Müller HW. Collagen matrix in spinal cord injury. J Neurotrauma. 2006; 23:422–36. [PubMed: 16629627]
22. Stichel CC, Müller HW. The CNS lesion scar: new vistas on an old regeneration barrier. J Cell Tissue Res. 1998; 294:1–9.
23. Mescher AL, Neff AW. Limb regeneration in amphibians: immunological considerations. The Scientific World. 2006; 6:1–11.
24. Gould, SJ. Ontogeny and Phylogeny. Belknap Press; 1977.
25. Shaffer HB. Evolution in a paedomorphic lineage. II. Allometry and form in the Mexican ambystomatid salamanders. Evolution. 1984; 38:1207–18.
26. Brommer H, Brama P, Laasanen MS, Helminen HJ, Weeren PR, Jurvelin JS. Functional adaptation of articular cartilage from birth to maturity under the influence of loading: a biomechanical analysis. Equine Vet J. 2005; 37:148–54. [PubMed: 15779628]
27. Hunziker EB, Kapfinger E, Geiss J. The structural architecture of adult mammalian articular cartilage evolves by a synchronized process of tissue resorption and neoformation during postnatal development. Osteoarthritis Cartilage. 2007; 15:403–13. [PubMed: 17098451]
28. Jadin KD, Bae WC, Schumacher BL, Sah RL. Three-dimensional (3-D) imaging of chondrocytes in articular cartilage: growth-associated changes in cell organization. Biomaterials. 2007; 28:230–9. [PubMed: 16999994]
29. Holder N. An experimental investigation into the early development of the chick elbow joint. J Embryol Exp Morphol. 1977; 39:115–27. [PubMed: 886251]
30. Mitrovic D. Development of the diarthrodial joints in the rat embryo. Am J Anat. 1978; 151:475–85. [PubMed: 645613]
31. Khan IM, Redman SN, Williams R, Dowthwaite GP, Oldfield SF, Archer CW. The development of synovial joints. Curr Top Dev Biol. 2007; 79:1–36. [PubMed: 17498545]

32. Pacifici M, Koyama E, Shibukawa Y, Wu C, Tamamura Y, Enomoto-Iwamoto M, et al. Cellular and molecular mechanisms of synovial joint and articular cartilage formation. Ann N Y Acad Sci. 2006; 1068:74–86. [PubMed: 16831907]

33. Maden M. Intercalary regeneration in the amphibian limb and the rule of distal transformation. J Embryol Exp Morphol. 1980; 56:201–9. [PubMed: 7400743]

34. Muneoka K, Holler-Dinsmore GV, Bryant SV. Pattern discontinuity, polarity and directional intercalation in axolotl limbs. J Embryol Exp Morphol. 1986; 93:51–72. [PubMed: 3734687]

35. Roy S, Levesque M. Limb regeneration in axolotl: is it super-healing? Scientific World Journal. 2006; 6(Suppl 1):12–25. [PubMed: 17205184]

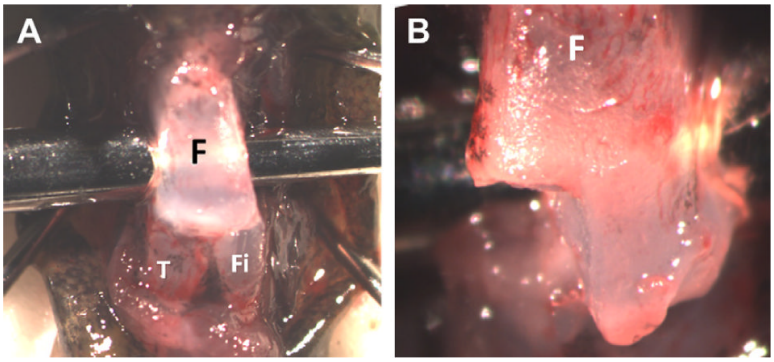

Fig. 1.
Arthrotomy of the axolotl femorotibial joint (A) showing the femur (F) tibia (T) and fibula (Fi). Resection of a single distal femoral condyle was completed by removal of epi physeal articular cartilage to the level of the metaphysis (B).

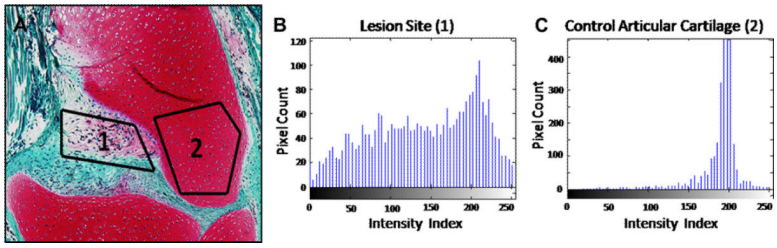

Fig. 2.

Selection of regions within the lesion site (A1) and the existing contralateral control femoral condyle (A2) used for image analysis. Histograms depicting distribution of red pixels within the repair tissue (B) and control articular cartilage (C). Pixel distributions were compared by calculating the KL divergence between sites.

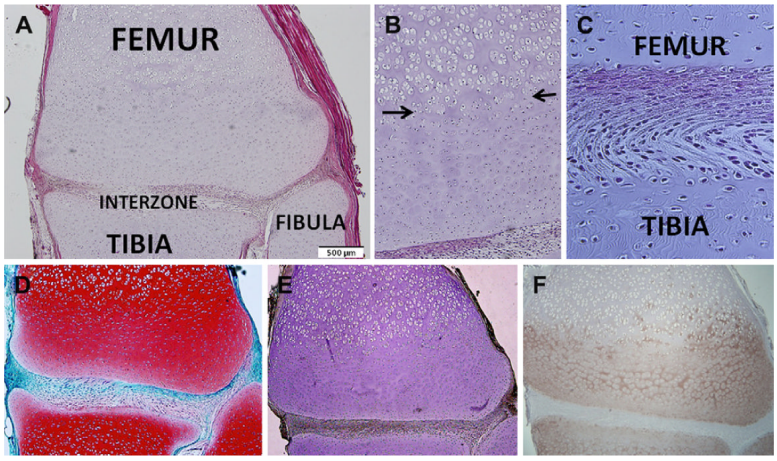

Fig. 3.

Anatomy of the axolotl femorotibial joint at (A) 4×, (B) 10× and (C) 20× magnification. Differences in chondrocyte morphology are evident at the junction of the epiphysis and metaphysis (B, arrows). A fibrous interzone-like tissue occupies the entire interarticular space, and appears adherent to articular surfaces (C). Positive Safranin-O staining is evident throughout the articular cartilage with faint staining in the interzone (D). Type I collagen immunostaining is found within the interzone-like tissue and cortical bone (E). Type II collagen immunostaining is present throughout the epiphyseal/articular cartilage, gradually decreasing at the epiphyseal-metaphyseal junction (F).

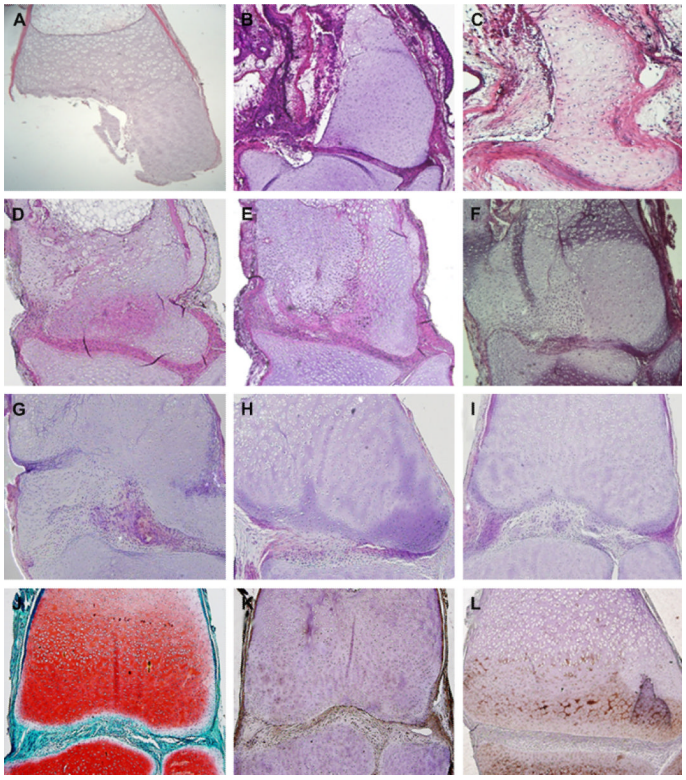

Fig. 4.

Axolotl healing response to medial condyle resection of the distal femur. H&E stained sections are shown at 0, 1, 2, 4, 6, 8, 12, 18, and 24 weeks post-surgery (A–I, respectively). Resection to the level of the metaphysis is confirmed at day 0 (A). At 8 weeks (F), cells which have a morphological resemblance to those found within the interzone-like tissue have populated the lesion site. Restoration of the articular cartilage was confirmed at 24 weeks with Safranin-O and immunohistochemistry for collagen I and collagen II (J–L, respectively).

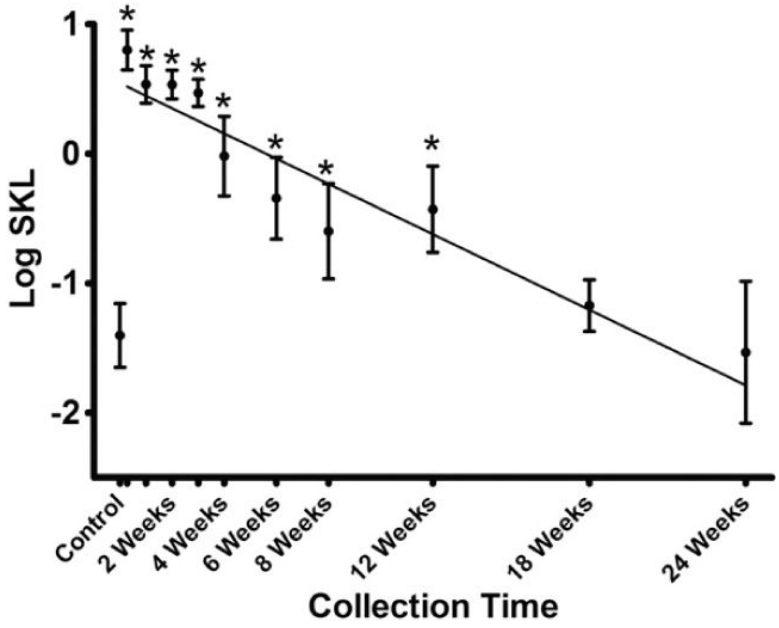

Fig. 5.

Symmetric KL divergence (SKL) between normal epiphyseal/articular cartilage and repair tissue stained with Safranin-O (mean ± 95% confidence interval). There was a strong negative correlation between collection time and SKL (r=−0.89, P < 0.01) as illustrated by a linear regression line (y=−0.09× + 0.54). * Indicates SKL values between normal and repair sites that are different (P < 0.05) from the SKL values in unoperated control femurs.